RSC Advances

ROYAL SOCIETY OF CHEMISTRY

www.rsc.org/advances

Liquid crystal droplets functionalized with charged surfactant and polyelectrolyte for non-specific protein detection

Lei Yang, Mashooq Khan, and Soo-Young Park*

School of Applied Chemical Engineering, Department of Polymer Science & Engineering, Polymeric Nano-material Laboratory, Kyungpook National University, #1370 Sangyuk-dong, Buk-gu, Daegu 702-701, Korea

*Corresponding author e-mail: psy@knu.ac.kr

Abstract: Monodisperse micrometer-sized 4-cyano-4′-pentylbiphenyl (5CB) droplets coated with ionic surfactant produced by a microfluidic technique were electrostatically functionalized with polyelectrolytes (PEs) at 5CB/aqueous interface, and the change in their configurational orientations was used for protein detection. Quarternized poly-4-vinylpyridine (QP4VP) and polystyrenesulfonate (PSS) (strong cationic and anionic PEs, respectively) were used for functionalization of the sodiumdodecylsulfate (SDS) and dodecyltrimethylammonium bromide (DTAB)-coated 5CB droplets ($5CB_{SDS}$ and $5CB_{DTAB}$), respectively, on which the charge densities (determined from the measured zeta potential) were controlled at their maximum values by adjusting the surfactant concentration. The radial (homeotropic) orientation of the $5CB_{SDS}$ and $5CB_{DTAB}$ droplets was changed to the bipolar (planar) orientation when the oppositely charged PE was adsorbed on the surfactant-coated droplets at concentrations not higher than 0.1 wt%, although it was retained when PE with the same charge was used. The adsorption of the PE may cause a decrease in the net electric field on the droplet surface. However, over-coating with high PE concentrations ($\geq$ 0.1 wt%) resulted in the radial orientation, probably due to the increased net electric field generated on the droplet surface by the over-coated PE. The QP4VP-functionalized $5CB_{SDS}$ droplets were then successfully utilized for protein detection with hemoglobin and bovine serum albumin as the model proteins. This new approach for functionalization of the interface between the LC and water may introduce a simple approach for developing LC-based biosensors.

Keywords: Liquid crystal, polyelectrolyte, surfactant, microfluidics, biosensor.

Introduction

Liquid crystal (LC) droplets dispersed in an aqueous medium become interesting stimuli-responsive materials when functionalized with smart materials at the LC/aqueous interface. They have also been used as a model system for studying particle rotations, optical momentum transfers, and optical vortex generation[1-5]. In recent years, LC droplets have emerged as a unique type of optical probe for detection of chemical and biological species[6-9], and the responses at their surfaces through changes in the director configuration are known to reflect the balance between the elasticity and the surface anchoring of the LC inside the droplets[10-12]. Thus, the adsorption of chemical and biological species at the LC/aqueous interface may disrupt the balance and trigger a configuration transition of the LC molecules inside the droplets, which can be easily observed using polarizing optical microscopy (POM). The naked LC droplets are usually unstable and tend to coalesce over time. For example, the sensitivity of naked LC droplets has been proven in sensing bacterial endotoxins but had poor stability [13]. In addition, the size of these LC droplets was not uniform, which can cause interference in detection, thus they are not suitable for use in biosensors.

A lot of effort has been made to produce uniform-sized and stable LC droplets using microfluidic techniques. The LC droplets produced with a microfludic device typically have bipolar and radial configurations (Figure 1), which depend upon the nature of the stabilizing agent that is used to prevent coagulation by reducing the interfacial tension of the LC droplets[14-15]. In the radial configuration, the LC molecules are oriented perpendicular to the droplet surface with a defect at the center of the droplet. This radial configuration corresponds to the homeotropic orientation of the LC in the flat surface. In the bipolar configuration, the LC mesogens are oriented parallel to the surface of the droplets with two diametrically opposite

surface point defects at the poles of the droplets. This bipolar configuration corresponds to a planar orientation of the LC in a flat surface[16-18]. A number of studies have reported that the spontaneous adsorption of surfactants and lipids at the LC/aqueous interface can stabilize the LC droplets in the aqueous solution and induce the bipolar-to-radial (B-R) configuration change[19-22]. Amphiphilic block copolymers were also used for stabilizing the LC droplets. For example, the 4-cyano-4′-pentylbiphenyl (5CB, a nematic LC at room temperature) droplets were coated with poly(acrylicacid)-b-poly(4-cyanobiphenyl-4′-undecyl acrylate) (PAA-b-LCP); the LC polymer (LCP) block anchors the LC while the PAA chains form a brush at the 5CB/aqueous interface. It was found that the PAA-b-LCP-coated-5CB droplets exhibit reversible radial and bipolar configurations at basic and acidic pH values, respectively. Furthermore, these pH-responsive LC droplets were further functionalized by immobilizing enzymes for detection of glucose, cholesterol, and urea [16, 23]. Similarly, the 5CB in a transmission electron microscopy (TEM) grid was coated with the block copolymers consisting of polyelectrolytes (PEs), such as quaternized poly(4-vinylpyridine) (QP4VP)[24], poly(styrenesulfonate) (PSS)[25], and poly(dimethylaminoethylmethacrylate) (PDMAEA)[26] for protein detection. A homeotropic orientation was observed when it was coated with QP4VP (strong cationic PE) and PSS (strong anionic PE) regardless of pH, while the orientation was found to be pH-dependent when it was coated with PAA (weak anionic PE) and PDMAEA (weak cationic PE) due to deprotonation and protonation of the pendant group above and below their pK_a values, respectively. A homeotropic-to-planar change was observed after the complexation of the PEs with oppositely charged proteins. Thus, the high net charge density on the LC droplet causes a radial (perpendicular) orientation and an R-B change occurs when the net charge density at the LC/aqueous interface decreases due to protein adsorption. However, the synthesis of such block

copolymers is a laborious task; hence, there is a strong need for comparatively simple approaches to functionalizing and stabilizing LC droplets for biosensor applications.

In this study, monodispersed micrometer-sized 5CB droplets produced by a microfluidic technique were electrostatically functionalized with polyelectrolytes (PEs) on the surface of the 5CB droplets that were already coated with oppositely charged surfactants, and the change in their configurational orientations was used for protein detection. Quarternized poly-4-vinylpyridine (QP4VP) and polystyrenesulfonate (PSS), (strong cationic and anionic PEs, respectively) were used for functionalization on sodiumdodecylsulfate (SDS) and dodecyltrimethylammonium bromide (DTAB)-coated 5CB droplets ($5CB_{SDS}$ and $5CB_{DTAB}$), respectively. An R-B configuration change was observed with a decrease in the charge density by coating the $5CB_{SDS}$ and $5CB_{DTAB}$ droplets with oppositely charged PEs at the LC/aqueous interface. The PE-functionalized 5CB droplets were then successfully utilized for demonstration of non-specific protein detection. This new approach for functionalization of the interface between the LC and water may introduce a simple approach for developing LC-based biosensors without synthesizing LC block copolymers, which have been synthesized for functionalizing its interface with PE blocks and anchoring LCs with LCP blocks in our previous studies[24-26].

Materials and Methods

Materials: Poly(dimethylsiloxane) (PDMS) kit (Sylgard 184, Dow Corning, USA, containing the pre-polymer and a cross-linker), 5CB (TCI Japan), PSS (M_w = 70,000 g/mol, Sigma-Aldrich), hemoglobin (Hglb, Sigma), bovin serum albumin (BSA, Sigma), BSA labeled with fluorescein isothiocynate (FITC-BSA, Sigma-Aldrich), diethyl ether (Sigma-Aldrich), pH buffer solutions (Samchun, Korea) were used as received. *N*,*N*-dimethylformamide (DMF, Sigma-Aldrich) was dried by distillation with added sodium sulfate. Milli-Q water (resistivity higher than 18.2 MΩ cm) was used in all experiments.

Synthesis of QP4VP: QP4VP was synthesized by using a reverse addition fragment transfer (RAFT) technique. 4-vinylpyridin (4-VP) (1.15 mL, 10 mmol), methoxycarbonylphenylmethyl dithiobenzoate (MCPDB, chain transfer agent (CTA)) (15.74 mg, 0.05 mmol), and DMF (1.115 mL) were added to a vial. The mixture solution was bubbled with dry nitrogen for 60 min. A Schlenk flask containing azobisisobutyronitrile (AIBN, 2.2 mg, 0.014 mmol) was evacuated for 60 min and the previously prepared solution of 4-VP and CTA in DMF was then introduced into the flask using a syringe needle that had been purged with N_2. The flask was placed in an oil bath thermostated at 80 °C for 4 h. The resulting polymer (poly(4-vinylpyridine) (P4VP)) was precipitated in diethyl ether. The number average molecular weight (M_n) and polydispersity index (PDI) were 16,000 g/mol and 1.17 respectively. The P4VP (0.062 g) was dissolved in DMF (5 mL), and CH_3I (0.18 mL) was then added dropwise into the polymer solution at 0 °C in darkness. The mixture was stirred at room temperature for 16 h. The mixture was finally added dropwise to diethyl ether to enable precipitation. The product (quarternized P4VP (QP4VP)) was filtered and dried in a vacuum oven at 40 °C.

Microfluidic chip fabrication: For the fabrication of microfluidic flow-focusing devices, PDMS

was prepared by mixing the pre-polymer and the cross-linker thoroughly at the recommended ratio of 10:1 (w/w) and degassing it for 40 min in a desiccator to remove the remaining air bubbles. The final mixture was poured onto a silicon wafer mold and cured inside an oven at 65 °C for 4 h before removing it from the structured silicon wafer. This patterned piece of PDMS was bonded to a pre-cleaned micro-slide glass using a short oxygen plasma treatment of 46 s using instrument Cute FC-10005, Femto Science Inc., Korea). Figure supplementary information (SI) 1 shows a schematic diagram of the microchip and the dimensions of the microfluidics channel. The width of the inlet channel, the orifice width, and the width of the outlet channel were 40, 40, and 160 µm, respectively, and the depth throughout all the channel was 100 µm. The channel walls and chip assembly were made hydrophilic by an oxygen plasma treatment. The channels were filled with water until the chip was used.

Preparation of the functionalized 5CB droplets: The 5CB droplets were formed by introducing the liquids to a microfluidic device via flexible plastic tubing (Norton, USA, i.d. 0.51 mm, o.d. 1.52 mm) attached to precision syringes (SGE Analytical Science, Australia) that were operated using digitally controlled syringe pumps (KDS 100 series, KD Scientific, USA). The flow of the fluids to the microfluidic channels was controlled using two independent syringe pumps. The dispersed and continuous phases in the microfluidic device were 5CB and an aqueous SDS (or DTAB) solution, respectively. The dispersed phase was supplied to the middle channel and the continuous phase was entered from the inlet channels on two sides. Both phases were combined at the junction and droplets were formed when the fluids crossed the neck of the channel. The typical flow rates used for droplet formation were 0.025 and 0.5 mL/h for the dispersed and continuous phases, respectively. The $5CB_{SDS}$ and $5CB_{DTAB}$ droplet formations were achieved by the spontaneous adsorption of the hydrophobic tail of the SDS and DTAB in

the 5CB molecules at the 5CB/aqueous interface. In order to optimize the density of SDS or DTAB molecules at the 5CB/aqueous interface, the SDS and DTAB aqueous solutions with different concentrations (C_{SDS} = 3.5 to 105 mM and C_{DTAB} = 23 to 98.6 mM) in the continuous phase were tested. The 100 µl of $5CB_{SDS}$ or $5CB_{DTAB}$ droplets in a chamber were exposed to 100 µl of aqueous QP4VP and PSS solutions, respectively at different concentrations (C_{QP4VP} = 0.000001 to 0.4 wt% and C_{PSS} = 0.00001 to 1 wt%). The QP4VP-coated $5CB_{SDS}$ ($5CB_{SDS/QP4VP}$) droplets were tested for protein detection at different concentrations Hglb (C_{Hglb}) and BSA (C_{BSA}) in PBS buffer after exposing to 100 µl of protein solution.

Characterization of LC droplets: The formation of on-chip droplets was imaged using a camera (STC-TC83USB-AS SenTech, Japan) attached to the inverted microscope. The POM images of the droplets were captured using a charge-coupled device (CCD) camera (STC-TC83USB-AS, SenTech, Japan) connected with a POM (ANA-006, Leitz, Germany). The fluorescence images was captured using fluorescent microscope (Nikon Eclipse,E600POL, Japan). The charge density on the 5CB droplets was studied using zeta potential measurement (Zatasizer Nano ZS90, Malvern Instruments Ltd., UK).

Results and Discussion

The bare 5CB droplets dispersed in an aqueous medium exhibit bipolar orientation, as reported elsewhere[23]. Figure 2a shows the POM images of the $5CB_{SDS}$ and $5CB_{DTAB}$ droplets exhibiting a radial orientation under crossed polarizers. The radial orientation was due to the adsorption of the hydrophobic tail of the surfactant into the 5CB molecules regardless of the nature of the hydrophilic head groups[21]. Past studies have shown that the interaction of surfactant tail and LC molecules largely dictates the orientation of the LC[20-21, 27]. For example, compression of the Langmuir monolayer of 4-octyl-4-cyanobiphenyl (8CB) and pentadecanoic acid (PDA) on water resulted in the vertical alignment of the 8CB[22]. This alignment of the 8CB was attributed to the interaction between the 8CB molecules and the tail of the PDA. Bare LC droplets in water are not stable and coalesced due to high surface tension on the surface, so that coating with materials which lower the surface tension is necessary to get uniform and stable droplets. Uniform sized $5CB_{SDS}$ and $5CB_{DTAB}$ droplets were achieved at $C_{SDS} \geq 3.5$ mM and $C_{DTAB} \geq 23$ mM, respectively using a microfluidics technique. At concentrations lower than these values, the droplets coalesced due to the high surface tension. The maximum amounts of the adsorbed surfactants on the 5CB droplets were studied using the zeta potentials. Figure 2b shows the zeta potentials of the $5CB_{SDS}$ and $5CB_{DTAB}$ droplets with respect to the concentrations of the SDS (C_{SDS}) and DTAB (C_{DTAB}) aqueous solutions used for coating. The anionic charge density of the $5CB_{SDS}$ increases with an increase in C_{SDS} reaching a saturation value of −45.32 at $C_{SDS} = 52$ mM. Similarly the cationic charge density of the $5CB_{DTAB}$ increases with an increase in C_{DTAB} until the saturation level of +36.21 at $C_{DTAB} = 62$ mM. The slightly lower saturation value for the zeta potential of the $5CB_{DTAB}$ than that of the $5CB_{SDS}$ may be due to the bulky head group of DTAB. Thus, the $5CB_{SDS}$ and $5CB_{DTAB}$ droplets coated at $C_{SDS} = 52$ mM and $C_{DTAB} = 62$ mM,

respectively, were used for all the experiments unless otherwise noted.

Response of $5CB_{SDS}$ to QP4VP: Figures 3a and b show the POM images of the $5CB_{SDS/QP4VP}$ droplets prepared at different values of C_{QP4VP} under crossed polarizers and the zeta potential of the $5CB_{SDS/QP4VP}$ droplets as a function of C_{QP4VP}, respectively. The initial radial orientation without QP4VP coating is maintained at C_{QP4VP} = 0.000001 wt% (Figure 3ai). At C_{QP4VP} = 0.00001 wt%, the orientation of a few droplets appears to change from radial to bipolar (R-B change) (Figure 3aii). The R-B change becomes more pronounced at C_{QP4VP} = 0.0001 and 0.001 wt% (Figures 3aiii and iv). At C_{QP4VP} = 0.01 wt%, the radial orientation appears again in a few droplets (Figure 3avi). This radial orientation becomes more evident with further increases of C_{QP4VP} to 0.1 and 0.4 wt% (Figures 3avi and viii). This R-B change at low C_{QP4VP} concentrations ($C_{QP4VP} \leq$ 0.001 wt%) and the B-R change with a further increase in C_{QP4VP} ($C_{QP4VP} \geq$ 0.01 wt%) is likely to be due to the increased charge density at the 5CB/aqueous interface by QP4VP. QP4VP is a strong cationic PE that has electrostatic attractions with oppositely charged head groups of SDS. These electrostatic interactions between them would reduce the net charge density to the balanced state causing the bipolar orientation at low QP4VP concentrations ($C_{QP4VP} \leq$ 0.001 wt%). However, the additional coating with QP4VP would increase the net cationic charge density causing the radial orientation to occur again at high QP4VP concentrations ($C_{QP4VP} \geq$ 0.01 wt%). This proposed charge state was monitored by zeta potential measurement (Figure 3b). The initial zeta potential of the $5CB_{SDS}$ droplets (−45 mV) changed to ~ 0 (C_{QP4VP} = ~ 0.001 wt%), positive values (C_{QP4VP} = 0.01 wt%), and saturated +32 ($C_{QP4VP} \geq$ 0.4 wt%). The R-B change occurred at low zeta potential values between −12 and +12 mV. When a PSS (anionic, 0.1 wt%) solution was exposed to the $5CB_{SDS}$ (Figure 3aviii) for comparison, the initial radial orientation is preserved because of the charge repulsion between

the pendent groups of PSS (anionic charge) and head groups of SDS (anionic charge), which prevents adsorption of the PSS chains on the $5CB_{SDS}$. These results confirm that the R-B and B-R change with increasing C_{QP4VP} is due to the adsorption of the QP4VP on the $5CB_{SDS}$ through electrostatic interactions.

Response of $5CB_{DTAB}$ to PSS: Figure 4a shows the POM images of the $5CB_{DTAB/PSS}$ droplets prepared at different values of C_{PSS} under crossed polarizers. The initial radial configuration was preserved at C_{PSS} = 0.0001 wt% (Figures 4ai). At C_{PSS} = 0.001 wt% (Figure 4aii), a slight R-B change was observed in a few droplets. The R-B change became more visible with a further increase in C_{PSS} (Figures 4aiii-v). Figure 4b shows the zeta potential of $5CB_{DTAB/PSS}$ droplets as a function of C_{PSS}. The initial positive zeta potential value (17 mV) decreased to ~ 0 mV (at C_{PSS} = 0.001 wt%) and was saturated at ~ -45 mV ($C_{PSS} \geq 1$ wt%) with an increase in C_{PSS}. Compared to the $5CB_{SDS/QP4VP}$ droplet, the $5CB_{DTAB/PSS}$ droplet shows the R-B change at relatively high values of C_{PSS} (0.01 wt%) without the B-R change by further increases in C_{PSS} (even at C_{PSS} = 1 wt%). This may be due to the bulky head group of DTAB, which may cause retardation in the electrostatic interactions. Another possible reason for the bipolar configuration even at high values of C_{PSS} may be that the hydrophobic and/or π-π interactions between the phenyl groups of 5CB and the benzene ring of PSS at the 5CB/aqueous interface create complex intermolecular forces that preserve the bipolar orientation. However, the detailed reasons should be studied in more systematic ways, which are beyond the current research scope of this article. When a QP4VP solution (cationic, 0.1 wt%) was introduced to the $5CB_{DTAB}$ droplets (cationic) for comparison, no R-B change was observed, as shown in Figure 4avi. This result confirms that the R-B change was due to the electrostatic interactions between the cationic DTAB and anionic PSS, which are similar to those of the $5CB_{SDS/QP4VP}$ droplets.

$5CB_{SDS/QP4VP}$ droplets for protein detection: It is found that the high charge density of the 5CB droplet can be obtained by coating PE on the oppositely charged surfactant-coated 5CB droplet. This charged droplet can be used for protein detection. In order to detect proteins, the pH of the system is important because the charge state of the tested protein is dependent on the pH of the protein solution[28]. The configuration of $5CB_{SDS/QP4VP}$ droplets was tested at different values of pH, as shown in Figure 5a. They exhibit the radial orientation at the tested whole number values of pH (2 – 12) (Figure 4a). Figures 5b and c show the POM images of the $5CB_{SDS/QP4VP}$ droplets prepared at C_{QP4VP} = 0.3 wt% when BSA and Hglb solutions (0.2 wt%) were injected at different pH values. The isoelectric points (PIs) of BSA and Hglb are 4.7 and 6.8, respectively. An R-B change was observed only at pH values above their PIs (pH $\geq$ 5 and $\geq$ 7 for BSA and Hglb solutions, respectively) with no R-B change at pH values below their PIs. Thus, this R-B change is due to the electrostatic interactions between the tested protein and cationic QP4VP[26]. This interaction can reduce the charge density at the 5CB/aqueous interface and cause an R-B change. In order to confirm that the R-B change was due to the electrostatic interaction, the 0.2 wt% aqueous solution of the BSA labeled with fluorescein isothiocynate (FITC-BSA) was tested with the $5CB_{SDS/QP4VP}$ droplets at pH = 3 and 7. Figure 6 shows the fluorescent images of the $5CB_{SDS/QP4VP}$ droplets after washing with a PBS buffer of the respective pH. The green color was clearly observed at pH 7, while black images were observed at pH 3 which indicates that the anionic charged FITC-BSA formed electrostatic interactions with the cationic charged QP4VP at pH 7 while no interaction occurred at pH 3 due to the same charges between the FITC-BSA and QP4VP. This result confirms that the change in 5CB orientation was due to the electrostatic interactions at 5CB/aqueous interface.

Sensitivity of $5CB_{SDS/QP4VP}$ droplets: The sensitivity of $5CB_{SDS/QP4VP}$ droplets was studied with different concentrations of the BSA and Hglb solutions. Figure 7 shows the POM images of the $5CB_{SDS/QP4VP}$ droplets under crossed polarizers at different values of C_{BSA} (Figure 7a) and C_{Hglb}

(Figure 7b). The pH of the tested proteins solution (pH = 7 and 9, for the BSA and Hglb solutions, respectively) was chosen above their PIs to have a negative net charge. The minimum protein detection limits were observed through the R-B change of the droplets. The initial radial configuration is preserved until C_{BSA} = 0.005 (Figure 7aii) and C_{Hglb} = 0.01 (Figure 7biii). A slight R-B change is observed at C_{BSA} = 0.01 and C_{Hglb} = 0.03 wt%, as shown in Figures 7aiii and 7biv. The R-B change becomes more prominent with an increase in the protein concentration. These results suggest that QP4VP can bind the proteins strongly via electrostatic interactions and induce the charge density at the 5CB/aqueous interface. This interaction may provide a new and simple method for protein detection.

Conclusion

The $5CB_{SDS}$ and $5CB_{DTAB}$ droplets produced using microfluidic technique were successfully coated with QP4VP and PSS respectively, via electrostatic interactions. The coating with oppositely charged PE induced the R-B configuration change. In particular, the B-R configuration change was also observed only for the $5CB_{SDS}$ droplets when the $5CB_{SDS/QP4VP}$ droplets were prepared with high concentrations of the oppositely charged QP4VP. The $5CB_{SDS/QP4VP}$ droplets were utilized for BSA and Hglb detection, which were used as model proteins. The proteins were successfully detected above their PI values using POM under crossed polarizers. This approach for the functionalization of the 5CB/aqueous interface may open a new way in developing LC-based biosensors without synthesizing LC block copolymers, which have been used for functionalizing its interface with PE blocks and anchoring LCs with LCP blocks in our previous studies.

Acknowledgment: This work was supported by the National Research Foundation of Korea

(NRF-2011-0020264 and NRF-2014R1A2A1A11050451).

Supplementary Information: Image and schematic of the microfludic chip used in this study

References

1. M. Nikkhou, M. Skarabot, S. Copar, M. Ravnik, S. Zumer and I. Musevic, *Nat Phys*, 2015, **11**, 183-187.
2. P. Hsu, P. Poulin and D. A. Weitz, *Journal of Colloid and Interface Science*, 1998, **200**, 182-184.
3. S. Juodkazis, M. Shikata, T. Takahashi, S. Matsuo and H. Misawa, *Applied Physics Letters*, 1999, **74**, 3627-3629.
4. T. A. Wood, H. F. Gleeson, M. R. Dickinson and A. J. Wright, *Applied Physics Letters*, 2004, **84**, 4292-4294.
5. E. Brasselet, N. Murazawa, H. Misawa and S. Juodkazis, *Physical Review Letters*, 2009, **103**, 103903.
6. D. YuanChen and Y. ZhongQiang, *Chin Sci Bull*, 2013, **58**, 2557-2562.
7. V. J. Aliño, J. Pang and K.-L. Yang, *Langmuir*, 2011, **27**, 11784-11789.
8. Q.-Z. Hu and C.-H. Jang, *Soft Matter*, 2013, **9**, 5779-5784.
9. S. J. Woltman, G. D. Jay and G. P. Crawford, *Nature Material*, 2007, **6**, 929-938.
10. P. Drzaic, *Molecular Crystals and Liquid Crystals Incorporating Nonlinear Optics*, 1988, **154**, 289-306.
11. T. Bera and J. Fang, *Journal of Materials Science and Chemical Engineering*, 2014, **2**, 1-7.
12. V. K. Gupta, J. J. Skaife, T. B. Dubrovsky and N. L. Abbott, *SCIENCE*, 1998, **279**, 2077-2080.
13. I. H. Lin, D. S. Miller, P. J. Bertics, C. J. Murphy, J. J. de Pablo and N. L. Abbott, *Science*, 2011, **332**, 1297-1300.
14. P. Poulin and D. A. Weitz, *Physical Review E*, 1998, **57**, 626-637.
15. O. Mondain-Monval, J. C. Dedieu, T. Gulik-Krzywicki and P. Poulin, *Eur. Phys. J. B*, 1999, **12**, 167-170.
16. M. Khan and S.-Y. Park, *Sensors and Actuators B: Chemical*, 2014, **202**, 516-522.
17. D. S. Miller and N. L. Abbott, *Soft Matter*, 2013, **9**, 374-382.
18. P. Malik and K. K. Raina, *Optical Materials*, 2004, **27**, 613-617.
19. J. M. Brake, M. K. Daschner, Y. Y. Luk and N. L. Abbott, *SCIENCE*, 2003, **302**, 2094-2097.
20. J. M. Brake, A. D. Mezera and N. L. Abbott, *Langmuir*, 2003, **19**, 6436-6442.
21. N. A. Lockwood, J. J. de Pablo and N. L. Abbott, *Langmuir*, 2005, **21**, 6805-6814.
22. M. Barmentlo and Q. H. F. Vrehen, *Chemical Physics Letters*, 1993, **209**, 347-351.
23. J. Kim, M. Khan and S.-Y. Park, *ACS Applied Materials & Interfaces*, 2013, **5**, 13135-13139.
24. M. Omer and S.-Y. Park, *Anal Bioanal Chem*, 2014, 1-10.
25. M. Omer, M. Islam, M. Khan, Y. Kim, J. Lee, I.-K. Kang and S.-Y. Park, *Macromol. Res.*, 2014, **22**, 888-894.
26. M. Omer, M. Khan, Y. K. Kim, J. H. Lee, I.-K. Kang and S.-Y. Park, *Colloids and Surfaces B: Biointerfaces*, 2014, **121**, 400-408.
27. Y.-Y. Luk and N. L. Abbott, *Curr. Opin. Colloid Interface Sci.*, 2002, **7**, 267-275.
28. O. Hayden, P. A. Lieberzeit, D. Blaas and F. L. Dickert, *Advanced Functional Materials*, 2006, **16**, 1269-1278.

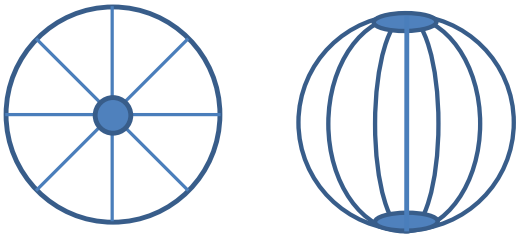

(a) (b)

Figure 1. (a) Radial and (b) bipolar configurations of an LC droplet.

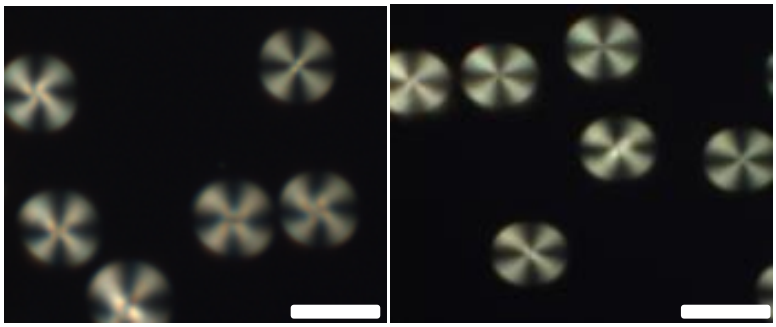

(a)

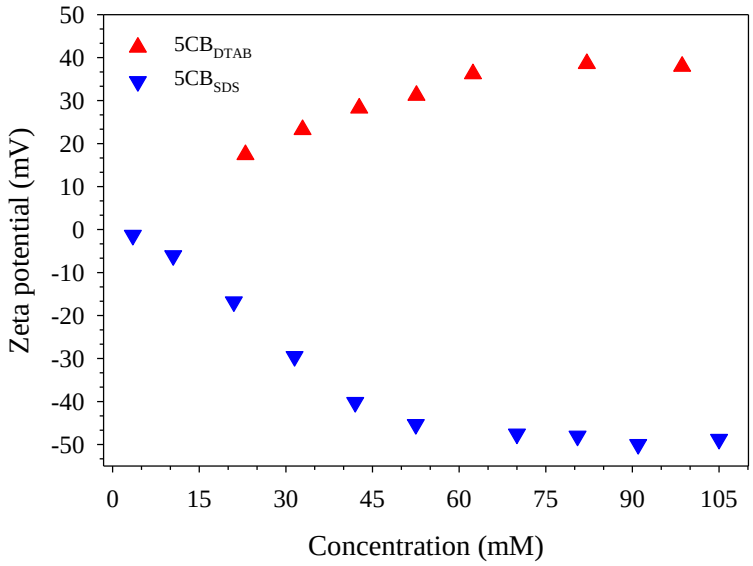

(b)

Figure 2. (a) POM images of (i) $5CB_{SDS}$ and (ii) $5CB_{DTAB}$ droplets; (b) zeta potentials of $5CB_{DTAB}$ and $5CB_{SDS}$ as a function of the surfactant concentration; the scale bars in (a) are 100 μm.

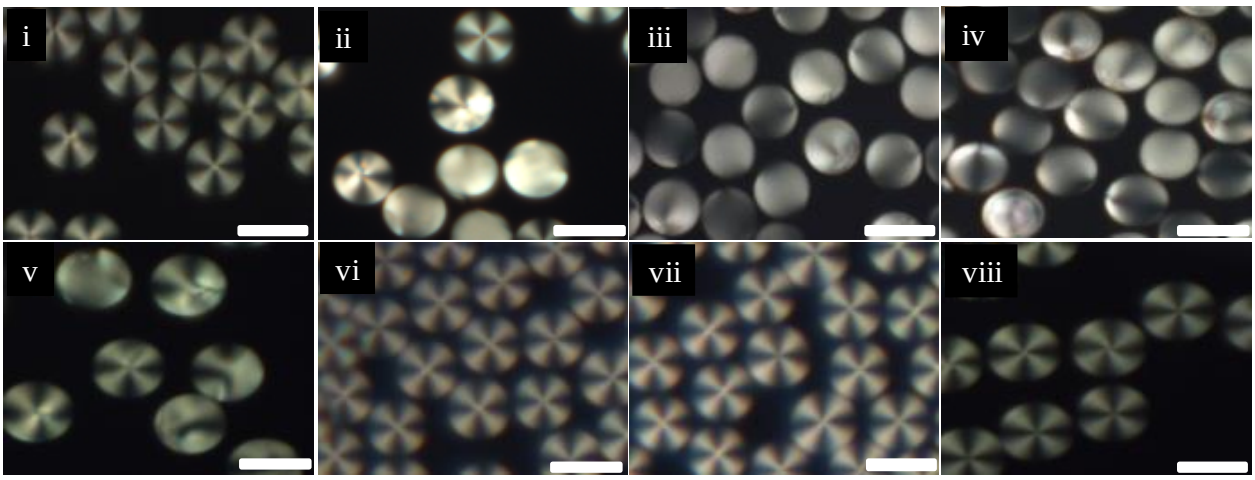

(a)

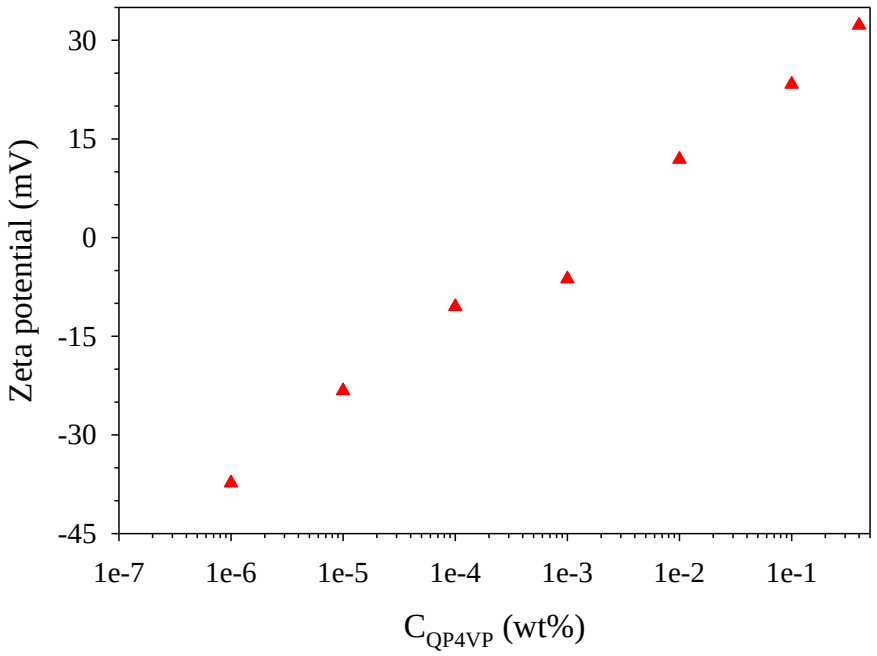

(b)

Figure 3. (a) POM images of $5CB_{SDS/QP4VP}$ droplets at C_{QP4VP} = (i) 0.000001, (ii) 0.00001, (iii) 0.0001, (iv) 0.001, (v) 0.01, (vi) 0.1, and (vii) 0.4 wt%, and (viii) $5CB_{SDS/PSS}$ droplets in an 0.1 wt% PSS solution; the scale bars are 100 µm. (b) Zeta potential of $5CB_{SDS/QP4VP}$ droplets as a function of C_{QP4VP}.

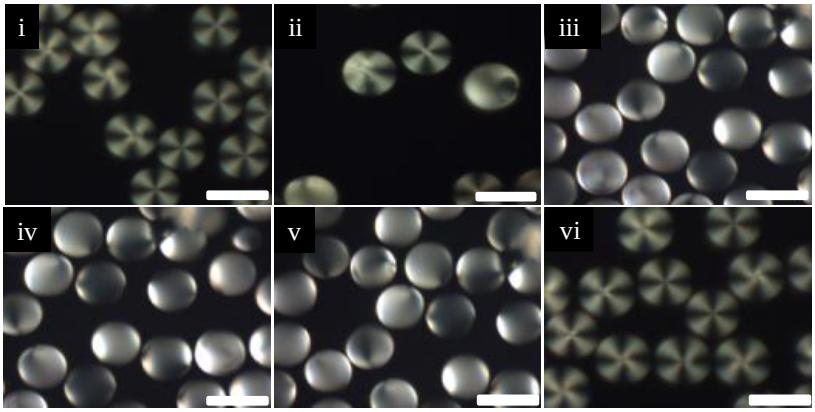

(a)

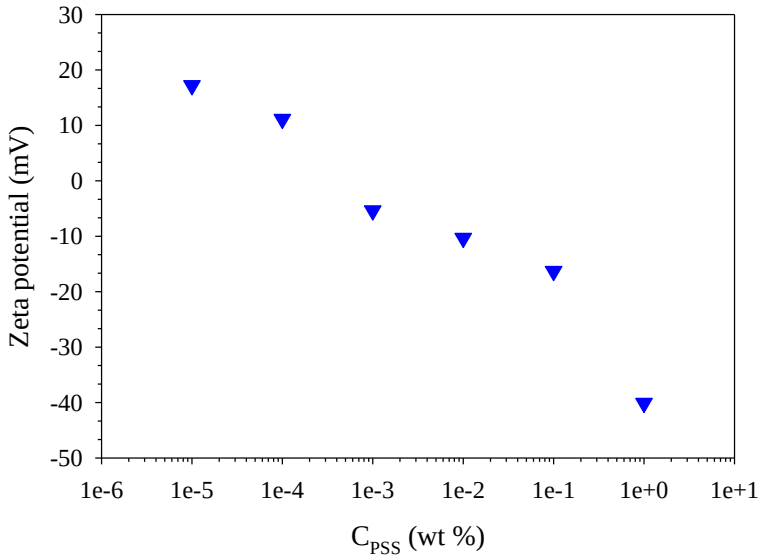

(b)

Figure 4. (a) POM images of $5CB_{DTAB/PSS}$ droplets at C_{PSS} = (i) 0.0001, (ii) 0.001, (iii) 0.01, (iv) 0.1, and (v) 1 wt%, and (vi) $5CB_{DTAB}$ droplets in a 0.1 wt% QP4VP solution; the scale bars are 100 μm, (b) zeta potential of $5CB_{DTAB/PSS}$ droplets as a function of C_{PSS}.

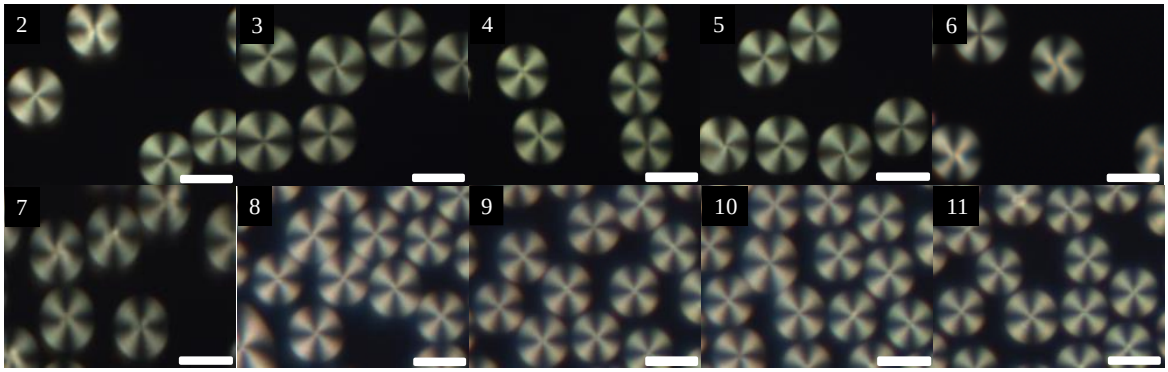

(a)

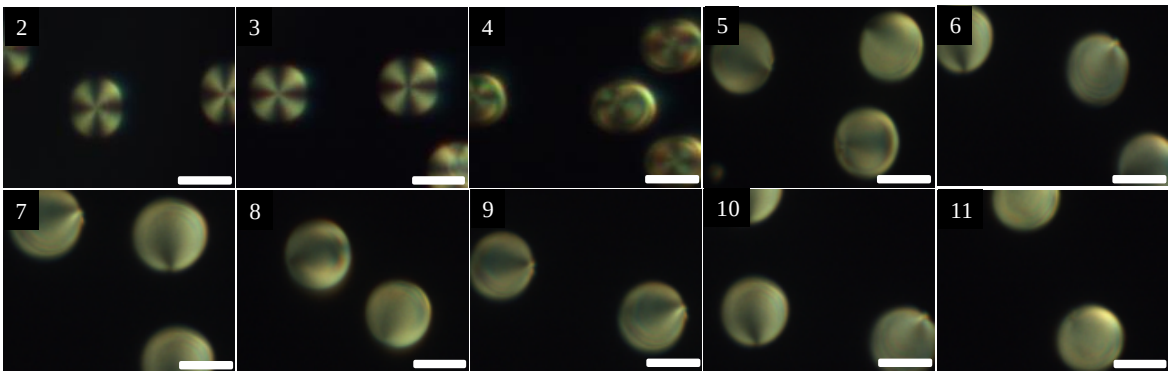

(b)

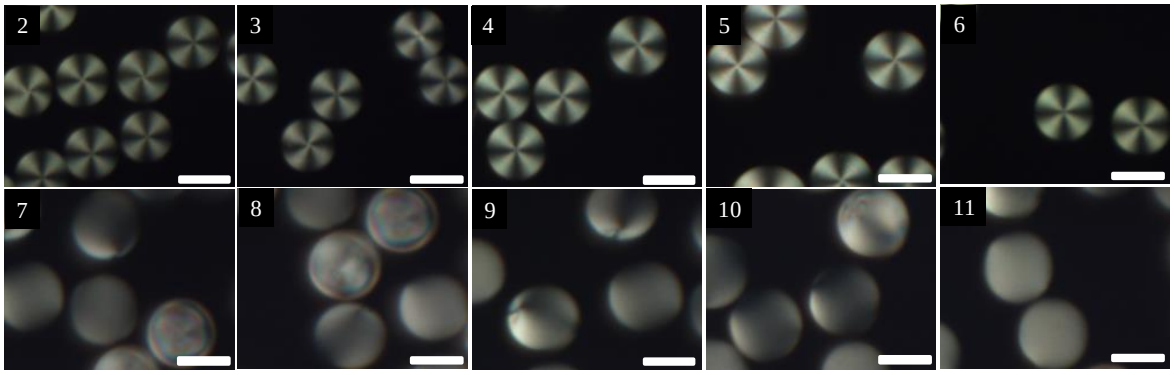

(c)

Figure 5. POM images of the $5CB_{SDS/QP4VP}$ droplets prepared at C_{QP4VP} = 0.3 wt% (a) without proteins, and with 0.2 wt% solutions of (b) BSA and (c) Hglb, in PBS buffer at different values of pH; the digit in figures represents the pH of the solution; the scale bars are 100 μm.

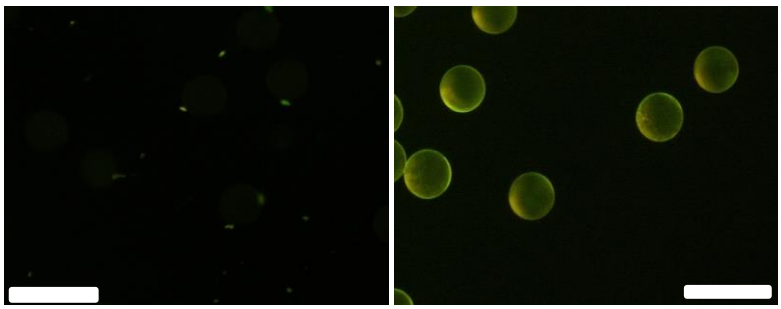

Figure 6. Fluorescence images of $5CB_{SDS/QP4VP}$ in 0.2 wt% FITC-BSA aqueous solution at pH = 3 (left) and 7 (right). The scale bars are 100 μm.

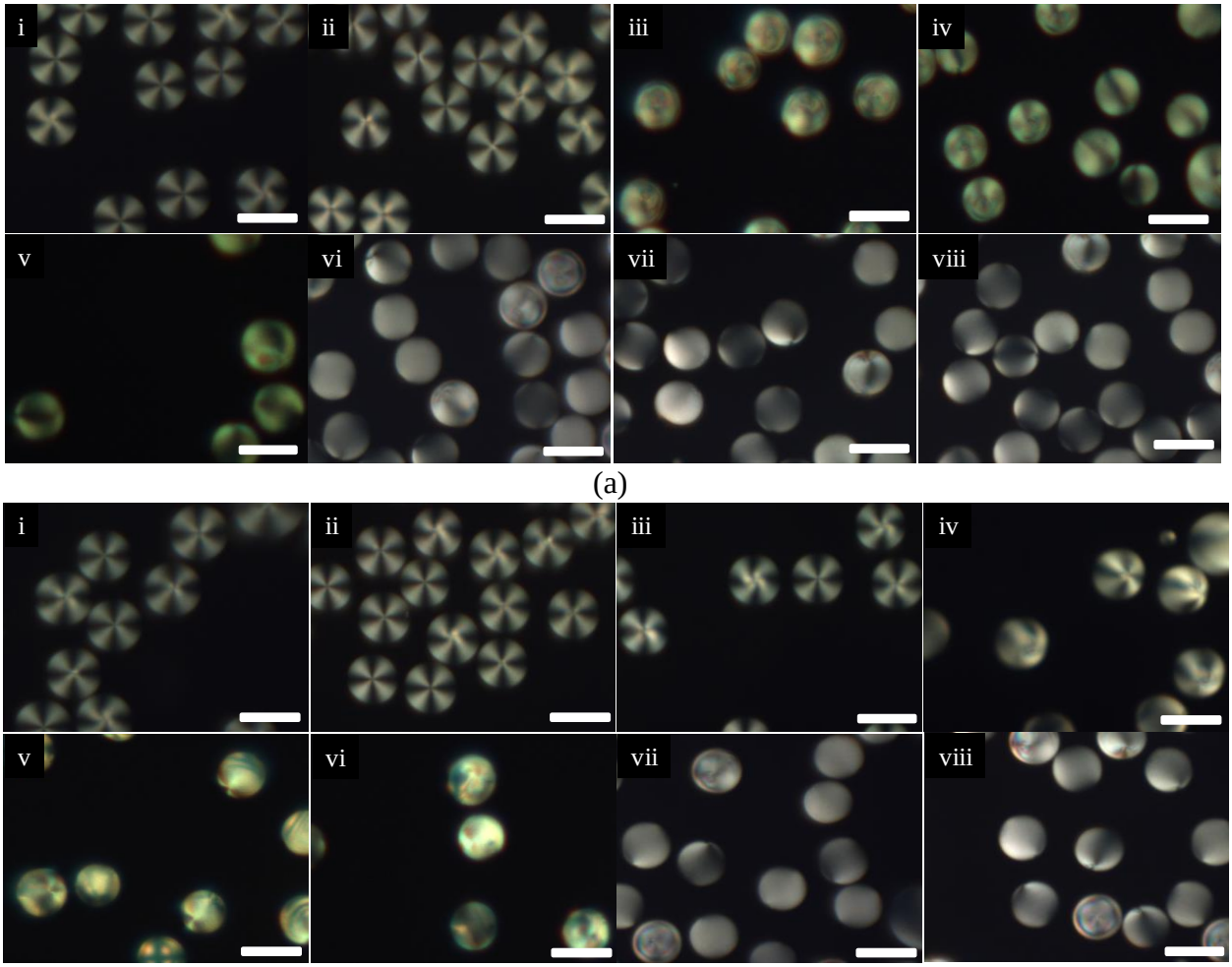

Figure 7. POM image of $5CB_{SDS/QP4VP}$ droplets at (a) C_{BSA} = (i) 0.001, (ii) 0.005, (iii) 0.01, (iv) 0.03, (v) 0.05, (vi) 0.08, (vii) 0.1, and (viii) 0.015 wt% and (b) C_{Hglb} = (i) 0.001, (ii) 0.005, (iii) 0.01, (iv) 0.03, (v) 0.05, (vi) 0.06, (vii) 0.08, and (viii) 0.1 wt%.

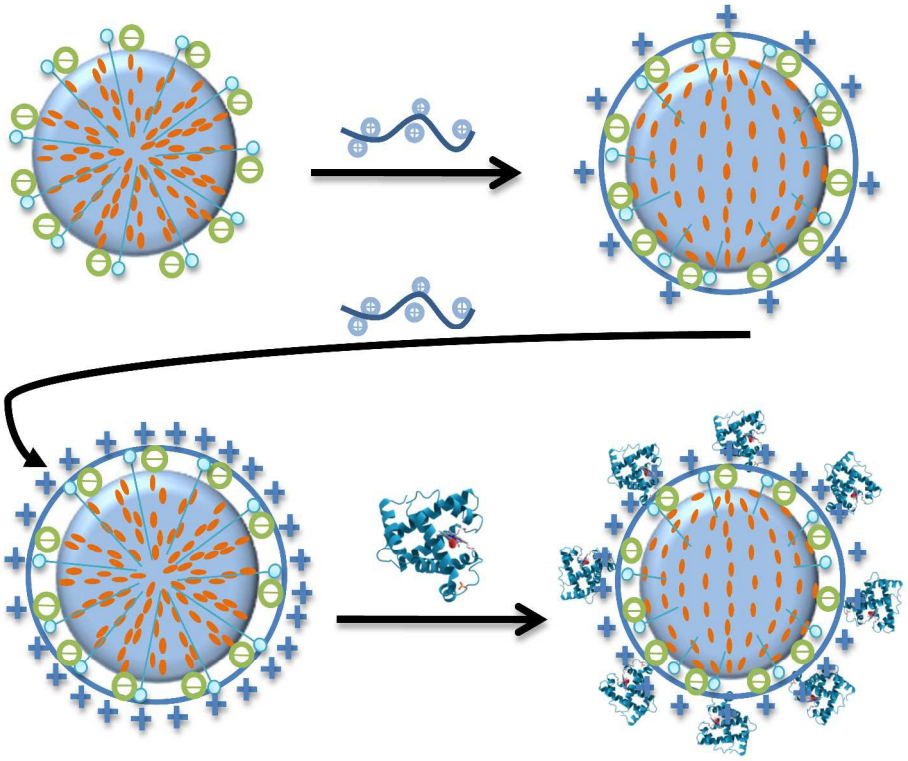

The $5CB_{surfactant}$ droplets were coated with polyelectrolytes for utilization of non-specific protein detection.